Physics of Fluids

Local anisotropy of laboratory two-dimensional turbulence affects pair dispersion

Cite as: Phys. Fluids **31**, 025111 (2019); https://doi.org/10.1063/1.5082851
Submitted: 25 November 2018 . Accepted: 19 January 2019 . Published Online: 13 February 2019

H. Xia, N. Francois, B. Faber, H. Punzmann, and M. Shats

Physics of Fluids ARTICLE scitation.org/journal/phf

Local anisotropy of laboratory two-dimensional turbulence affects pair dispersion

Cite as: Phys. Fluids 31, 025111 (2019); doi: 10.1063/1.5082851
Submitted: 25 November 2018 • Accepted: 19 January 2019 •
Published Online: 13 February 2019

H. Xia,[1,a)] N. Francois,[1] B. Faber,[2] H. Punzmann,[1] and M. Shats[1]

AFFILIATIONS

[1]Research School of Physics and Engineering, The Australian National University, Canberra, ACT 2601, Australia
[2]Department of Physics, University of Wisconsin-Madison, Madison, Wisconsin 53706, USA

[a)]hua.xia@anu.edu.au

ABSTRACT

Experimental investigation of particle pair separation is conducted in two types of laboratory two-dimensional turbulence under a broad range of experimental conditions. In the range of scales corresponding to the inverse energy cascade inertial interval, the particle pair separation exhibits diffusive behaviour. The analysis of the pair velocity correlations suggests the existence of coherent bundles or clusters of non-diverging fluid particles. Such bundles are also detected using a recently developed topological tool based on the concept of braids. The bundles are observed as meandering streams whose width is determined by the turbulence forcing scale. In such locally anisotropic turbulence, the particle pair dispersion depends on the initial particle separation and on the width of the bundles.

I. INTRODUCTION

Theoretical prediction of the inverse energy cascade by Kraichnan in 1967[1] opened the field of two-dimensional (2D) turbulence with applications ranging from atmospheric physics[2,3] to laboratory and industrial flows. While initially two-dimensional turbulence was thought as a mathematical abstraction, it turned out to be a robust physical mechanism observed in flows which are not intuitively perceived as 2D.[4,5] Laboratory experiments[6–10] and numerical simulations (e.g., Refs. 11 and 12) have confirmed Kraichnan's predictions of the two inertial ranges, below and above the forcing wave numbers: the inverse energy cascade range, $E_k \propto k^{-5/3}$ at wave numbers smaller than the forcing k_f, and the direct entropy cascade, $E_k \propto k^{-3}$ at $k > k_f$. Later, a 2D version of the Kolmogorov 4/5 law which relates the third-order structure functions for the velocity fluctuations to the separation distance in 2D turbulence has also been confirmed in laboratory experiments.[9,10] Overall, there is an agreement between theory, numerical simulations, and laboratory experiments on the main Eulerian statistics of 2D turbulence such as energy distribution between the scales.[13,14]

For problems related to the particle dispersion, such as mass transport, one needs to adopt a Lagrangian perspective and consider the fluid motion in the frame of moving fluid particles. The classical prediction by Richardson,[15] who considered a problem of a mean squared separation of initially close particles in a dispersing cloud, is that the diffusion coefficient should scale as $K = C_R R^{4/3}$, where C_R is a constant and R is the distance between two particles. Later, Obukhov[16] connected this result with Kolmogorov's distribution of energy in the turbulence spectrum and obtained a similar relation from dimensional reasoning. A Richardson-Obukhov law that follows from this reads $\langle R^2(t)\rangle = C_R \epsilon t^3$, where C_R is the Richardson constant and ϵ is the energy dissipation rate. The Richardson-Obukhov phenomenology describes the pair dispersion as a process in which initially close particles separate self-similarly and continuously for a long time, i.e., a process governed by a multi-scale dynamics in a *homogeneous isotropic* flow.

2D turbulence in laboratory is generated electromagnetically in layers of electrolytes,[6,7] in soap films,[17–19] and more recently, on the surface of a liquid perturbed by Faraday waves.[20,21] All these types of turbulence support the inverse energy cascade. It has recently been shown that in the case of the wave-driven turbulence, the underlying Lagrangian structure of the flow is dominated by locally anisotropic bundles of fluid trajectories.[22] Such anisotropic bundles should be responsible for modifications to the self-similar dispersion expected in isotropic turbulence and may bring important deviations from the classical Richardson-Obukhov law.

Here we study experimentally the pair dispersion statistics in both electromagnetically driven and in Faraday-wave driven turbulence at Reynolds numbers typical for quasi-2D laboratory turbulence, $Re \leq 200$. We show that the presence of locally anisotropic bundles substantially modifies the pair dispersion at modest Reynolds numbers.

II. EXPERIMENTAL SETUP AND DATA ANALYSIS

In the reported experiments, turbulence is produced using two different methods described in Refs. 23 and 24. In the first method, turbulence is generated electromagnetically in layers of electrolytes.[7] In the second method, it is driven by parametrically excited surface waves or Faraday waves.[21,25]

Electromagnetically driven turbulence (EMT) is produced in layers of electrolytes by generating an electric current across the fluid cell (square container 30 × 30 cm) placed above an array of permanent magnets.[9,10,24,26] A double layer configuration is used to reduce the bottom dissipation and 3D effects.[27] In this case, a 4 mm thick layer of Na_2SO_4 water solution is placed on top of a 4 mm layer of a heavier, non-conducting, low-viscosity fluid (FC-3283). The Lorenz $J \times B$ force produces horizontal vortices which interact with each other, generating complex 2D flows. By changing the current density J, one can control the degree of turbulence development and the energy injected into the flow at the scale which is approximately equal to the distance between the magnets (9 mm in this experiment), the forcing scale L_f.

The second method of turbulence generation, the Faraday wave turbulence (FWT), was recently discovered on the surface of vertically vibrated liquids.[20,21] The motion of particles on the surface perturbed by parametrically excited Faraday waves reproduces remarkably well the fluid motion in 2D turbulence. This method relies on the ability of waves to generate vorticity at the fluid surface.[25,28,29] In these experiments, Faraday waves are generated in a 180 mm diameter circular container filled with water. The container is shaken vertically at the frequency of 60 Hz at the peak-to-peak acceleration in the range of $a = (1–2)g$, where g is the gravitational acceleration.

The experimental parameters for different experiments analyzed in this paper are shown in Table I, where U^2 is the kinetic energy of the flow (U is the rms of the horizontal velocity fluctuations) and T_L is the Lagrangian autocorrelation time, which will be discussed later. All flows, listed in Table I, are turbulent. The Reynolds number, $Re = UL_f/\nu$ (L_f is the forcing scale, and ν is the kinematic viscosity), is in the range of 25–200. Results on the single particle dispersion in the same experiments[24] suggest that the finite boundary size effects are negligible. The single particle dispersion D_{exp}, the kinetic energy of the flow U^2 and the Lagrangian time T_L were measured independently. The measured dispersion

TABLE I. Experimental parameters for different experiments analyzed. The forcing in the EMT experiments is controlled by the current, while in the FWT experiments, it is controlled by the vertical acceleration.

Label	Forcing	U^2 (m^2/s^2)	L_f (mm)	T_L (s)
EMT1	0.4×10^3 A/m^2	7.6×10^{-6}	9	1.9
EMT2	0.6×10^3 A/m^2	2×10^{-5}	9	1.6
EMT3	0.8×10^3 A/m^2	3.1×10^{-5}	9	1.2
EMT4	1.2×10^3 A/m^2	5.1×10^{-5}	9	1
FWT1	60 Hz, 1.0g	1.6×10^{-4}	4.4	0.27
FWT2	60 Hz, 1.2g	3.2×10^{-4}	4.4	0.17
FWT3	60 Hz, 1.6g	1.02×10^{-3}	4.4	0.1
FWT4	60 Hz, 2.0g	1.83×10^{-3}	4.4	0.08

confirms Taylor's particle dispersion law for unbounded system: $D = U^2 T_L$.

The kinetic energy spectra of these flows show a 2D inverse energy cascade range scaling of $E_k \sim k^{-5/3}$.[10,21,23,24] Examples of the spectra are shown in Fig. 1. The energy injected into the system at $k_f = 2\pi/L_f$ is transferred to larger scales forming $k^{-5/3}$ spectra. The increase in forcing (injected energy) leads to the increase in total horizontal kinetic energy of the flow, but the shapes of spectra remain unchanged (Fig. 1). All flows considered in this paper are in the steady state; the spectra do not change over time.

Although both flows show the Kolmogorov-Kraichnan spectra, the nature of the forcing is different in these two experimental setups. For the EMT experiments, the forcing vortices are initially generated at fixed positions determined by the array of permanent magnets. These vortices are then pushed around and randomised by shearing and sweeping effects.[30] In the FWT experiments, Faraday waves have been shown to act as quasi-particles, or oscillating solitons.[31–33]

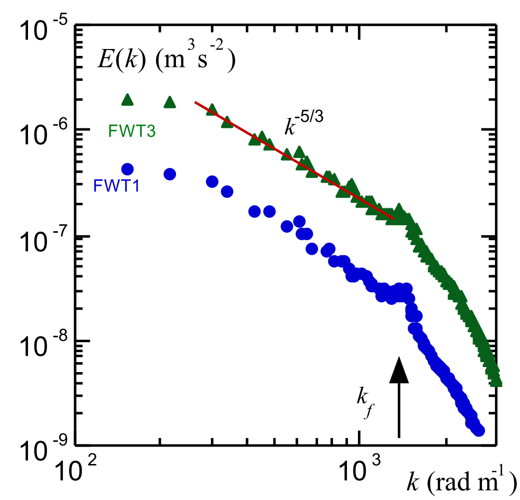

FIG. 1. Kinetic energy spectra of turbulence at two different forcing levels in Faraday wave turbulence. Vertical accelerations are $a = 1g$ (blue circles) and $a = 1.6g$ (green triangles).

Vorticity is injected into the flow at the oscillon scale[25] and randomized by the turbulent flow. The motion of oscillons is related to that of the tracer particles on the surface as recently reported.[33]

In both experiments, the motion on the fluid surface is visualized by placing 50 μm polyamid particles (specific gravity SG = 1.03) on the water surface. The use of surfactant and plasma treatment of the particles ensures homogeneous distribution of the tracer particles. The particle motion is captured using a high-resolution fast camera (Andor Neo sCMOS) as described in Refs. 21 and 24. In the EMT experiments, an area of 10×10 cm^2 was recorded at 30 fps, while in the FWT experiments, an area of 8×8 cm^2 was recorded at the speed of up to 120 fps. The velocity fields are obtained using particle image velocimetry (PIV).[10] To investigate the pair dispersion, particle trajectories are generated by numerical integration of the Lagrangian equation of motion, $d\mathbf{x}(t)/dt = \mathbf{u}(\mathbf{x}, t)$. Here $\mathbf{x}(t)$ is a particle 2D coordinate, and $\mathbf{u}(\mathbf{x}, t)$ is the measured velocity field. Typically 4×10^5 particles advected by the flow are tracked using the fourth order Runge-Kutta method. Direct tracking of particles using particle tracking velocimetry (PTV) has also been employed.[24] In this case, the seeding density of the imaging particles is lower than in the PIV experiments, to improve the accuracy of the particle tracking. The domain of the measurement and the observation time of the experiments are carefully chosen to avoid any boundary effects on the velocity measurements. In all these experiments, no spectral condensation is observed.[10,21]

The two-dimensionality of the EMT flows has been investigated both numerically[34] and experimentally.[27] It has been shown that in the double-layer configuration, the flow is two dimensional. In the FWT experiments, the particle motion on the surface is three dimensional. However, as has been shown before, the statistics of the horizontal motion exhibit properties of two-dimensional turbulence. Here we characterize the dimensionality of the surface flow using the divergence of the horizontal velocity field defining the 2D compressibility parameter as[35]

$$C = \frac{\langle(\partial_x v_x + \partial_y v_y)^2\rangle}{\langle(\partial_x v_x)^2\rangle + \langle(\partial_x v_y)^2\rangle + \langle(\partial_y v_x)^2\rangle + \langle(\partial_y v_y)^2\rangle}, \tag{1}$$

where v_x, v_y are the two-dimensional velocity components at the surface. C $\geq$ 0.5 is indicative of a compressible 2D flow. For the FWT experiments presented in this paper, the compressibility parameter averaged over 1 Faraday wave period is small (~0.1–0.2), close to the value obtained in the quasi-2D EMT experiments. With an increase in the averaging time the

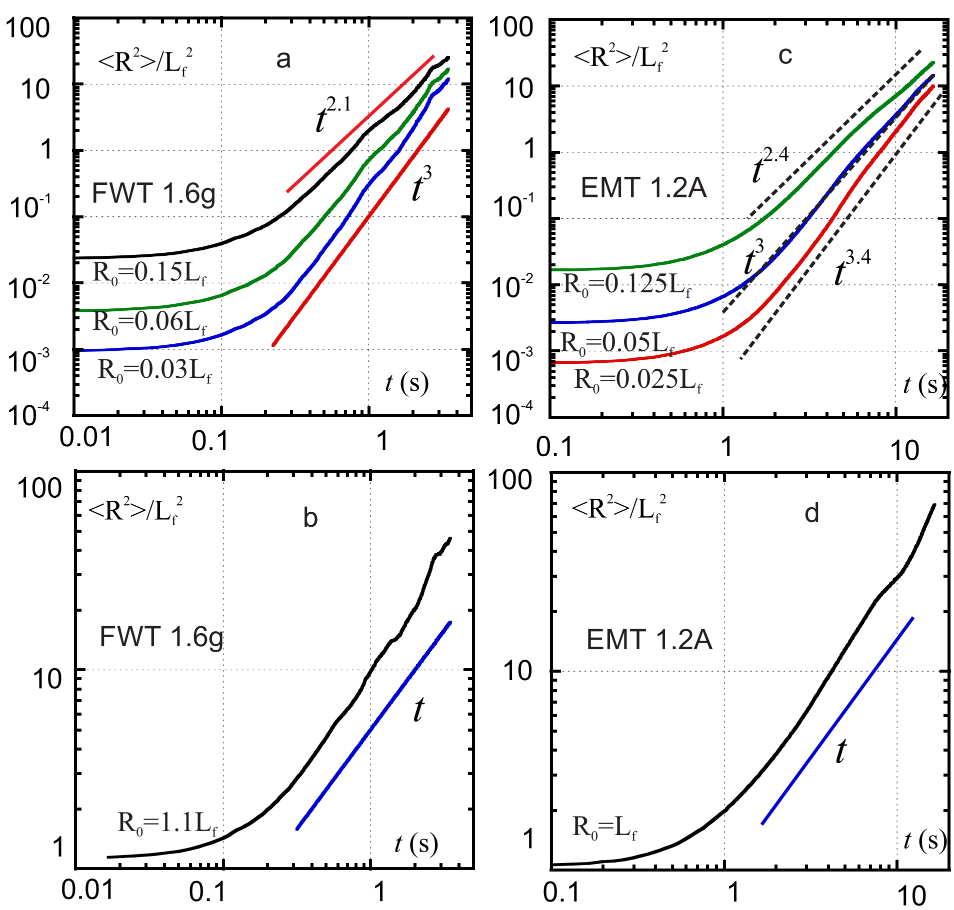

FIG. 2. Mean squared separation of the tracer particles in pairs as a function of time for three initial separations measured in (a) FWT, and (c) EMT. The dotted lines represent power laws of (a) $t^{2.1}$ and t^3, and (c) $t^{2.4}$, t^3, and $t^{3.4}$. Mean squared separation of the tracer particles in pairs for the initial separation of $R_0 \simeq L_f$ in (b) FWT and (d) EMT.

compressibility parameter converges to an even lower value of $C \approx 0.05$. Thus, both the EMT and FWT flows can be considered as good laboratory models of 2D turbulence.

III. PAIR SEPARATION AND THE EXIT-TIME STATISTICS

The mean squared distance (MSD) between particles in a pair at time t, $\langle R^2(t)\rangle$, is the statistical average of the squared distances R^2 between two particles which are initially (at $t = t_0$) separated by a distance R_0.

We compute the MSD of pairs for different initial separations using trajectories reconstructed from the PIV data. Similarly to previously published results,[36] the MSD of the pairs is strongly dependent on the initial separation. When R_0 is small compared with the forcing scale, $R_0 < L_f$, the MSD exhibits a power law $\langle R^2\rangle \propto t^b$, as shown in Figs. 2(a) and 2(c). Such scaling laws are observed in all the experiments, both in the EMT and in the FWT. At larger separations, $R_0 \geq L_f$, the MSD behavior changes to $\langle R^2\rangle \sim t$, Figs. 2(b) and 2(d), showing a diffusive dispersion law.

This diffusive separation is also observed in the analysis of the particle trajectories obtained using the direct PTV method. In Fig. 3, the MSD in experiment FWT2 is shown for an initial separation of $R_0 \sim L_f$. The number of pairs used in this analysis is 2000. The scaling at long time is close to $\langle R^2\rangle \propto t$, the same as the one shown in Figs. 2(b) and 2(d).

The results of Figs. 2(b), 2(d), and 3 do not show the Richardson-Obukhov law for the pair separation. In the inverse energy cascade range $r > L_f$, the Richardson-Obukhov law predicts that the pair separation should scale with t as $\langle R\rangle^2 \sim t^3$. However, our experimental results show a diffusive behaviour $\langle R\rangle^2 \sim t$ for both the trajectories obtained using the direct PTV technique and the numerically integrated trajectories using the PIV data.

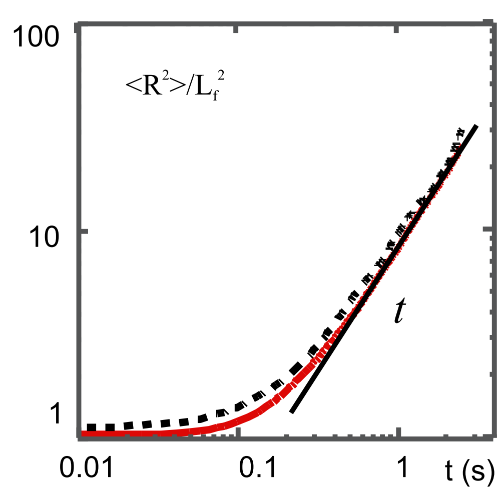

FIG. 3. Mean squared separation of the tracer particles in pairs as a function of time for the direct PTV data. The measurements are performed in the FWT (f_0 = 60 Hz, vertical acceleration $a = 1.2g$). The MSD obtained from PIV data shown in Fig. 2(b) is reproduced here as a dashed line.

The exit time statistical analysis was proposed in Refs. 36 and 37 as an alternative analysis tool to evaluate the pair dispersion in turbulence. It relies on the statistically averaged time t_{ex} it takes for particles within the pairs to separate from R_0 to βR_0. $\beta = 1.2$ is usually chosen for most of the analyses performed in the literature.[38] For a Richardson scaling of t^3, the exit time should scale as $t_{ex} \propto R_0^\gamma$ with $\gamma = 2/3$ for scales larger than L_f. $\gamma = 0.83$ was previously reported from laboratory experiments of 2D turbulence.[38] Here we perform the exit time statistical analysis using several values of β.

Figure 4 shows the results using $\beta = 1.2$, 1.5, and 2, respectively. In Fig. 4(a), the normalized exit time $t_{ex}/(R_0/L_f)^{2/3}$ is shown as a function of the initial separation (the initial separation R_0 is normalized by L_f). The $\beta = 1.5$ case shows a reasonable plateau consistent with a Richardson law for scales R_0/L_f between 2 and 8. No plateau is observed for the other cases despite a weak variation in β. For all the experiments shown in Table I, with $\beta = (1.2–2)$, we find the exit time scales as $t_{ex} \propto R_0^\gamma$, with $\gamma = (0.4–0.7)$. These values of γ correspond to $b = (2.8–5)$, where b is the scaling parameter in $\langle R^2(t)\rangle \sim t^b$.

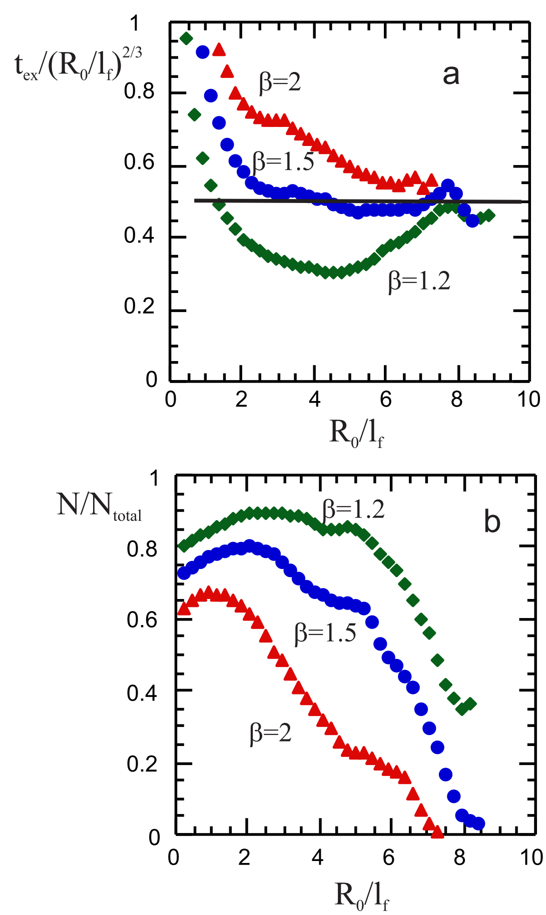

FIG. 4. (a) The normalised exit time $t_{ex}/(R_0/l_f)^{2/3}$ and (b) the number of trajectories in the exit time analysis, for three different β. The measurements are performed in the FWT2.

In Fig. 4(b), we show the ratio N/N_{total}, where N is the number of pairs of trajectories separated by more than β times the initial separation, and N_{total} is the total number of trajectories with the same initial separation. Note that in all the experiments, N_{total} is more than 10^4. The particles are tracked for a long time: more than 40 times the Lagrangian velocity autocorrelation time for the FWT experiments and 15 times for the EMT experiments. It can be seen in Fig. 4(b) that for the range where the Richardson scaling is observed ($2 \lesssim R_0/L_f \lesssim 8$) for the β = 1.5 case, the number of trajectories pairs drops from 80% to 20%.

The result in Fig. 4 shows a distinct difference between the exit time analysis and the MSD analysis. In the exit time analysis, many particle pairs, initially separated by R_0, do not play a significant role. Indeed, only the particle pairs separated by more than βR_0 really contribute to the statistically averaged exit time t_{ex}.

Here the analysis of the number of trajectories considered in the exit time statistics reveals the statistics is biased towards strongly diverging pairs and all the non-diverging particles pairs play no role. We will show in Sec. IV that accounting for the non-diverging particle pairs is essential to reveal physical mechanisms of the pair separation in 2D laboratory turbulence.

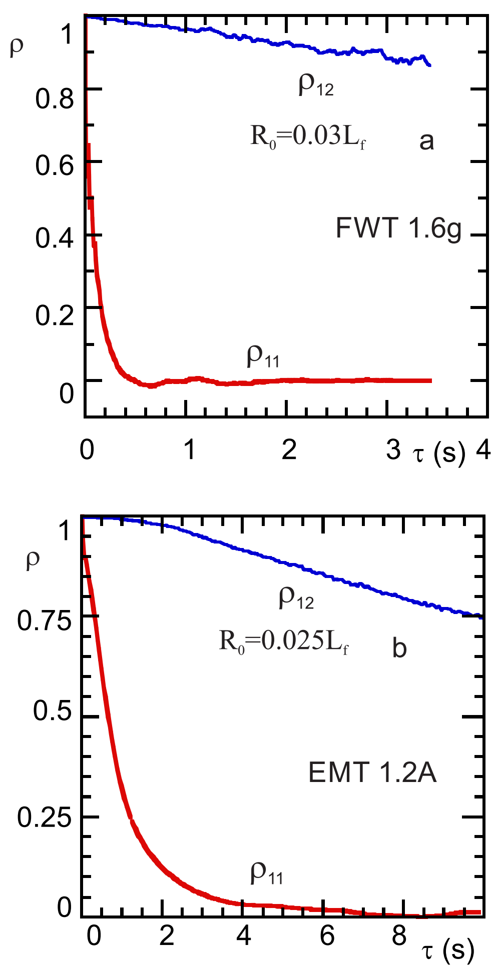

FIG. 5. Autocorrelation (ρ_{11}) and cross correlation functions (ρ_{12}) measured in (a) FWT3 and (b) EMT4 experiments.

IV. DIRECTIONAL CROSS CORRELATION FUNCTIONS

To evaluate the importance of non-diverging particle pairs in the flows, it is instructive to ask the following question: how different are the Lagrangian velocity correlation functions along the trajectories for (i) a single particle and (ii) two particles in a pair in 2D turbulence? The single particle velocity *autocorrelation* function is computed as $\rho_{11}(\tau) = \langle \vec{u}(t_0 + \tau) \cdot \vec{u}(t_0)\rangle/\sigma^2$, where σ^2 is the velocity variance. The Lagrangian velocity integral time is given by the integral of the function $T_L = \int_0^\infty \rho_{11}(\tau)d\tau$. The directional velocity *cross correlation* function[39] of particles pair is computed as $\rho_{12}(\tau) = \langle \vec{u}_1(\tau) \cdot \vec{u}_2(\tau)\rangle/\sigma^2$. The directional cross correlation function differs from a standard cross correlation function which characterises the similarity between two signals separated by a time lag. Here $\rho_{12}(\tau)$ measures to what degree the velocity of the 1st particle is correlated with that of 2nd particle at time τ, while the two particles are initially separated by R_0.

The two correlation functions measured in fully developed 2D turbulence are shown in Fig. 5. For the FWT experiment, the autocorrelation function drops exponentially, leading to an autocorrelation time of $T_L \sim 0.1$ s, Fig. 5(a), while the velocities of particles in the pairs are correlated for much longer time, $\tau > 4$ s. Similar observations are made in the EMT, Fig. 5(b). This suggests that a large number of pairs travel together for a long time without separating, while any individual particle quickly forgets its initial direction. This agrees with the conclusion of Ref. 40 which shows that the separation of particles in pairs is governed by rare, extreme events and the majority of initially close pairs are not dispersed.

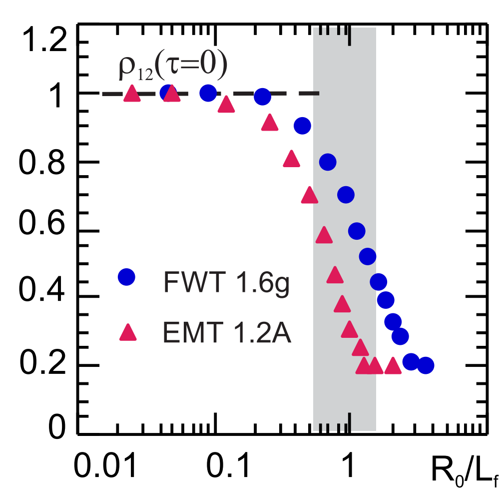

FIG. 6. The cross correlation of the pairs at the initial time, $\rho_{12}(t_0)$, as a function of the initial separation. Circles and triangles are for FWT 60 Hz 1.6g (L_f = 4.4 mm) and EMT 1.2 A (L_f = 9 mm) experiments, respectively.

To characterize the ensemble of non-diverging pairs, we compute the cross correlation functions for different initial distances R_0. The temporal behaviour of the functions is similar to that shown in Fig. 5. However, the initial correlation $\rho_{12}(0)$ at $\tau = 0$ changes substantially with the increase in the initial separation, Fig. 6. In the FWT experiments (circles in Fig. 6), at small initial separations, $\rho_{12}(0)$ is very close to 1. The cross correlation coefficient $\rho_{12}(0)$ drops substantially (by a factor of 5) in the range $R_0/L_f = [0.5, 1.5]$, until the velocity correlation reaches $\rho_{12}(0) \approx 0.2$ at $R_0 \approx 1.5L_f$. A similar trend is observed in the EMT experiments (triangles in Fig. 6). This suggests that non-diverging pairs exist in bundles which have a typical width between $0.5L_f$ and $1.5L_f$. Particles in pairs are decorrelated if the distance between them is comparable or larger than the forcing scale. This can also be interpreted as the lack of the correlation between fluid particles belonging to different coherent bundles.

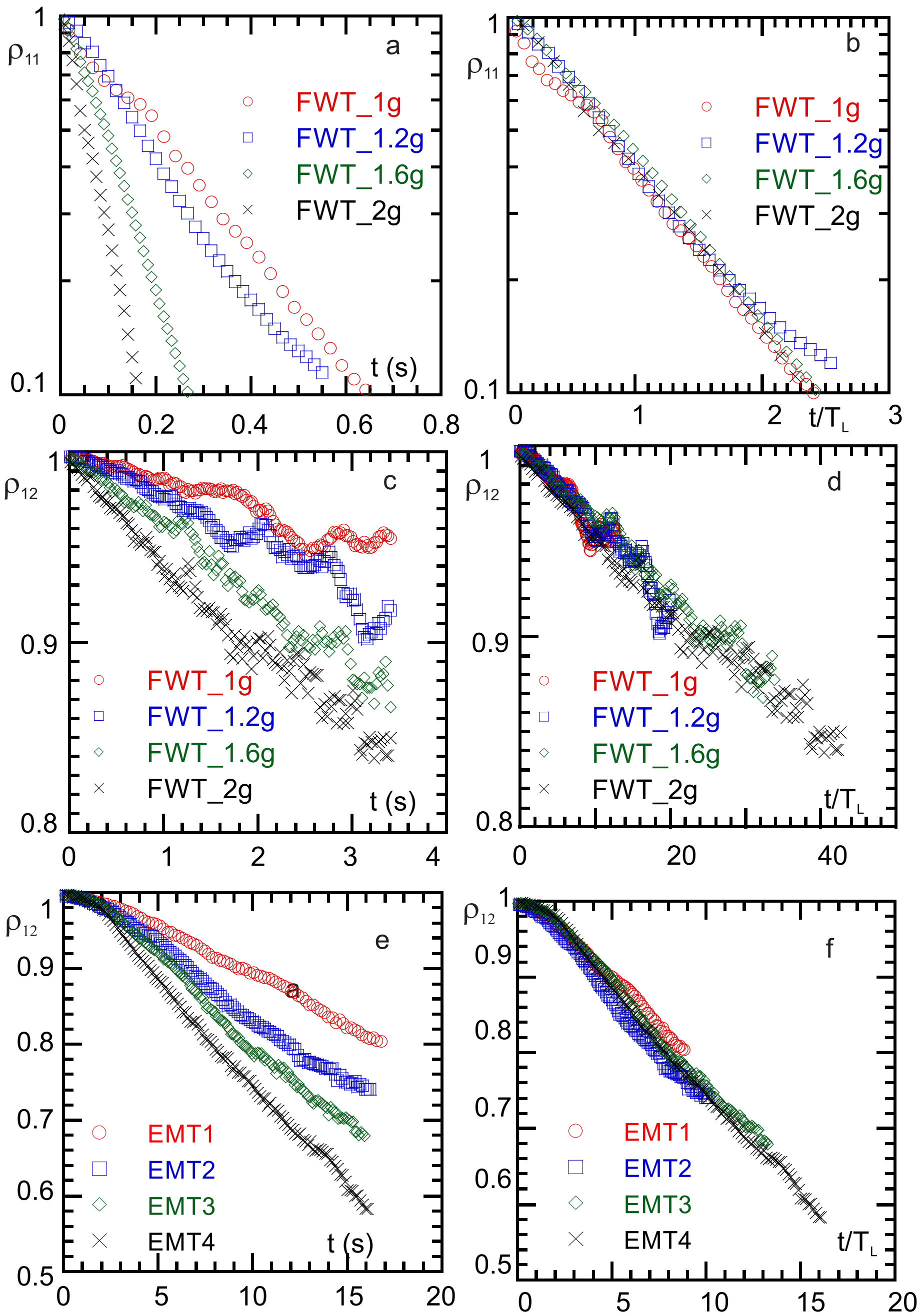

FIG. 7. [(a) and (b)] Autocorrelation functions of a single particle Lagrangian velocity, and [(c) and (d)] Lagrangian velocity cross correlation function of particles in the pairs [(a) and (c) versus time t and (b) and (d) versus t/T_L]. Measurements are performed in the FWT experiments at the driving frequency of f_0 = 60 Hz at different vertical accelerations a = (1–2)g, where g is the acceleration of gravity. Lagrangian velocity cross correlation function of particles in the pairs (e) versus time t and (f) versus t/T_L for the EMT experiments at different current 0.4 A–1.2 A.

The important role of the forcing scale in 2D turbulence can be further revealed by performing measurements of the velocity cross correlation functions in a broad range of turbulent kinetic energies. The kinetic energy stored in the broadband turbulent velocity fluctuations increases with the increase in the energy injected into the flow at the forcing scale. The single particle autocorrelation functions $\rho_{11}(\tau)$ are shown in Fig. 7(a) and have been studied in detail in Ref. 24. As the forcing is increased, the Lagrangian velocity autocorrelation time T_L gradually decreases. However if the correlation time is normalized by the Lagrangian integral time T_L, all autocorrelation functions collapse into one, Fig. 7(b).

A similar collapse is observed for the velocity pair cross correlation functions ρ_{12}, Figs. 7(c) and 7(d). Despite the fact that the pair cross correlation time is (50-70) times longer than the single particle velocity autocorrelation time, the cross correlation times expressed in the units of the Lagrangian integral time T_L appear to be the same regardless of the turbulence kinetic energy U^2. These conclusions are valid in both the EMT and FWT experiments. The results for the EMT experiments are shown in Figs. 7(e) and 7(f).

Similarly to the conclusion regarding the single particle dispersion,[24] the above results suggest that the pair decorrelation process is related to a single scale dynamics, namely, it is determined by the Lagrangian scale of 2D turbulence $L_L = UT_L$. The Lagrangian scale is related to the forcing scale, $L_L \approx 0.7L_f$, for a broad range of experimental conditions.[24] Here we re-plot the ratio of L_L/L_f for the experiments conducted in this paper in Fig. 8. It shows that $L_L/L_f \approx 0.75$ for all the data points, except for the one with the lowest kinetic energy. The deviation of the lowest energy point in Fig. 8 from the trend is probably related to the degree of turbulence (under-)development, as discussed in Ref. 23. Turbulence still plays an important role in this single-scale picture since the dispersion depends on the turbulent velocity fluctuations. The higher the kinetic energy of the flow U^2, the faster particle pairs separate from each other.

The effect of this single scale on the particle pair separation statistics is summarized in Fig. 8(b). The rate of particle pair separation α where $D \sim t^{\alpha}$ is shown as a function of the initial separation. It can be seen that α is strongly dependent on the initial separation R_0/L_f when R_0 is smaller than L_f. As shown in Fig. 8(b), α changes sharply from around 3 to 1. The dashed line is an exponential decay fit. For initial separation R_0 larger than L_L ($R_0/L_f \sim 0.8$), the particle pairs are not correlated and their pair dispersion is diffusive.

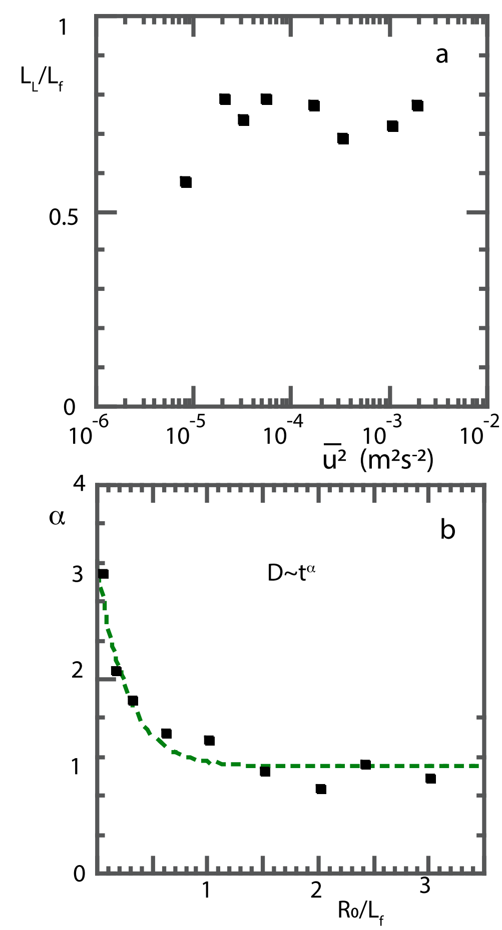

FIG. 8. (a) The ratio of L_L/L_f as a function of the total kinetic energy in the flow U^2. The corresponding parameter, U^2, T_L, and L_f are listed in Table I. (b) The rate of particle pair separation α where $D \sim t^{\alpha}$ as a function of initial separation R_0/L_f for FWT 1.6g experiment. The dashed line is an exponential decay fitting.

V. COHERENT BUNDLE ANALYSIS USING BRAIDS

To visualize particles in 2D turbulence which travel without any substantial dispersion, we employ a recently developed method of detection of coherent structures (here bundles) based on the notion of topological braids.[41,42] In the so-called braid approach, a coherent bundle can be identified as a set of trajectories which only entangle within themselves and does not interact, in a topological sense, with external trajectories; more details on topological entanglement of fluid particle trajectories can be found in Refs. 42 and 43.

In a nutshell, the degree of entanglement of trajectories within the flow can be quantified via a descriptor called the braiding factor.[43,44] The time evolution of the braiding factor can then be used for coherent structure detection. Measurements of the braiding factor of wave driven turbulent flows have recently been reported.[44] It has been shown that when trajectories are chosen such that their initial separation is larger than the forcing scale in 2D turbulence, their rate of entanglement grows exponentially in time at $t > 6T_L$.[44] Here, we use the time evolution of the braiding factor computed on subset of all the trajectories (including those separated by less than L_f) to detect the presence of coherent structure.

A visualisation based on the braid analysis is shown in Fig. 9. All trajectories in a given part of the turbulent flow appear as erratically entangled strands, Fig. 9(a). The braiding

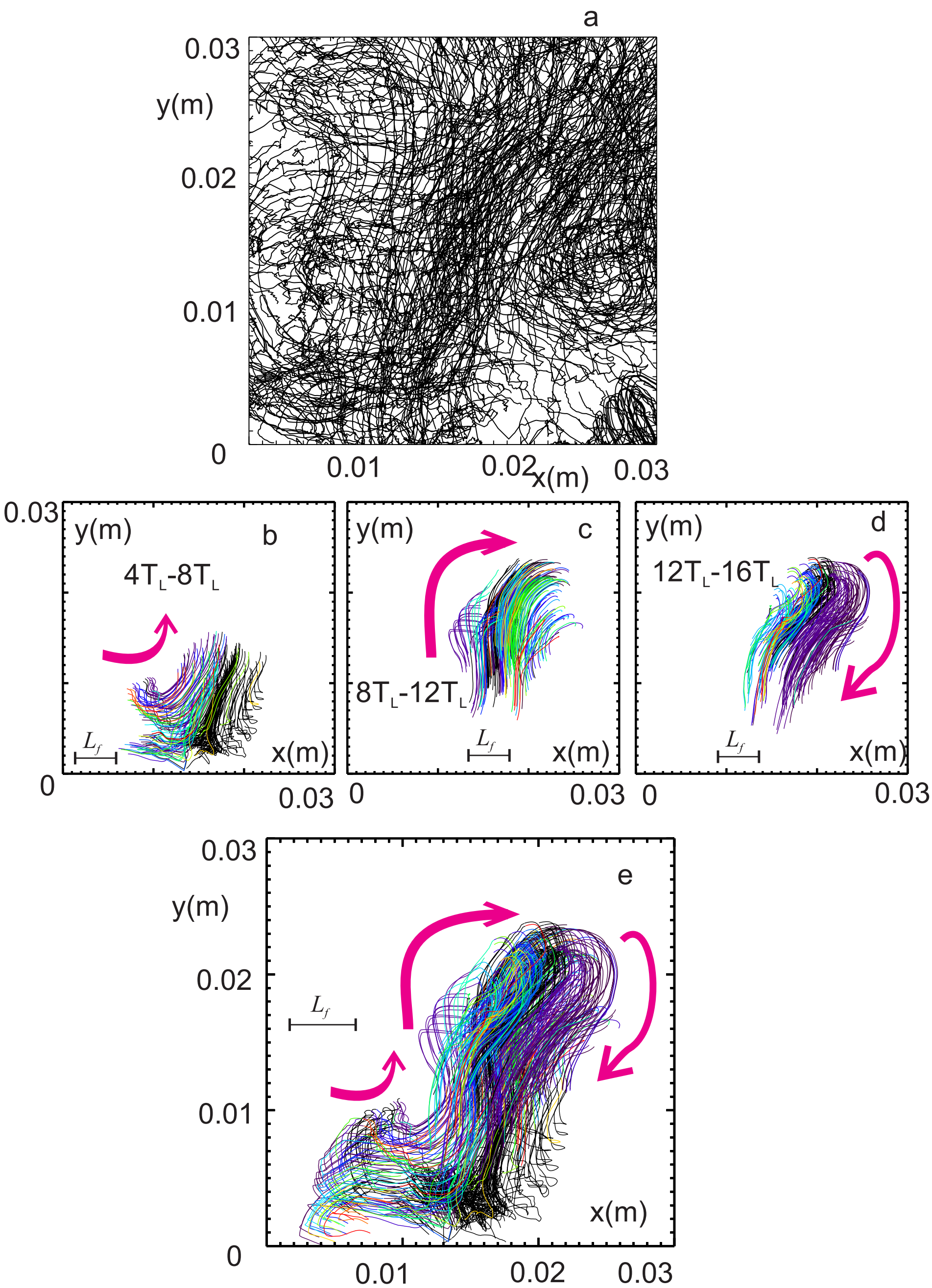

FIG. 9. Analysis of Lagrangian trajectories in FWT driven at f_0 = 60 Hz. The turbulence forcing scale is L_f = 4.4 mm. (a) A subset of Lagrangian trajectories (1% of all trajectories are shown for clarity). Coherent bundles detected from (a) at different time intervals (b) $(4–8)T_L$, (c) $(8–12)T_L$, (d) $(12–16)T_L$. (e) A coherent bundle identified for the time intervals $(0–16T_L)$ by overlapping coherent bundles obtained for $4T_L$ segments, including (b)–(d). The scale bar in panels (b)–(e) shows the forcing scale.

factor is computed using a random selection of 100 trajectories out of a total of about 600 trajectories. The braids analysis reveals that a very large number of trajectories closely follow each other for rather long periods of time. Those bundle of fluid trajectories have a typical with of L_f. Such a bundle is shown in Figs. 9(b)–9(d), it is tracked for $16T_L$. These coherent bundles experience occasional splitting into two bundles, yet most strands stay together untangled and execute complex collective motion, Fig. 9(e).

VI. DISCUSSION

Despite the long history of the subject, there are still many outstanding questions about pair dispersion in both 2D and 3D turbulence.[45–48]

In 3D turbulence experiments, it has been shown that a pair of particles separate ballistically, $\langle R^2(t)\rangle \sim t^2$ for varying initial separations.[49] It is concluded that, to observe a Richardson-Obukhov scaling regime, a large separation between the Lagrangian time scale and the observation time is required. However, it is difficult to confirm this in the laboratory, because it would require turbulence levels beyond the reach of current experiments. Turbulence at such levels would also be in excess of most practical situations.

For laboratory 2D turbulence, though a particle separation scaling close to $\langle R^2(t)\rangle \sim t^3$ was reported in seminal experiments on pair dispersion,[8] there are still numerous outstanding questions. For instance, as noted in Ref. 46, it is somewhat surprising that the experimental results of Ref. 8 show a t^3 scaling in the pair dispersion for separation distances within the entropy range. In addition, the behaviour of the Richardson parameter C_R in 2D flows remains a controversial issue.[8,37,50] The problem in finding a robust Richardson-Obukhov scaling in laboratory turbulence could be due to the fact that the pair dispersion occurs not as a multi-scale self-similar process as expected in an isotropic flow, but it is rather governed by the underlying structures of the flow. Clearly, such a process should be very different from the Richardson-Obukhov phenomenology and would require alternative models to be considered, such as those discussed in Refs. 50–52.

In the present experiments, directional cross correlation analysis of the particle pairs reveals the important roles played by non-diverging particles in laboratory 2D turbulence at Reynolds numbers ($Re = UL_f/\nu$) of the order of 100. This result has been connected to coherent structures that take the form of long-living bundles of fluid trajectories [Fig. 9(e)].

The importance of non-diverging pairs of particles in the statistics of laboratory 2D turbulence has been noted earlier. The evidence in support of the existence of clusters of non-diverging particle pairs has been presented by Sokolov and Reigada.[40] By analysing experimental data produced in the electromagnetically generated turbulence,[7] the authors concluded that the pair dispersion is connected with rare and extreme events and the majority of pairs in the flow belong to non-diverging clusters. Our experimental results are consistent with this earlier analysis and show that the particle pair dispersion is a process which depends on both the forcing scale L_f and on the average turbulent velocity fluctuations U^2. In these flows, we observe a diffusive behaviour of the pair dispersion when it is computed within the $k^{-5/3}$ range of the energy spectrum. Though the process is not self-similar, turbulence plays an important role by storing the kinetic energy in the inertial interval. An increase in the kinetic energy substantially speeds up the pair dispersion. The presence of bundles introduces a degree of anisotropy in the turbulent flows that prevents the direct application of Richardson-Obukhov relation between Eulerian and Lagrangian description. In this anisotropic turbulence, it would be interesting to have a theoretical model that would relate the diffusive behaviour observed in the pair dispersion with the inverse cascade process.

Finally, it should also be noted that the majority of laboratory experiments in 2D turbulence are performed at much lower Reynolds number Re than those modelled numerically.[7,8,10,21,23,38] While numerical simulations and theory focus on high Re, all laboratory experiments deal with flows at $Re = UL_f/\nu < 200$. Recently, new results on a 2D turbulent flow forced at even lower Reynolds numbers were reported.[53] As in this study, the Lagrangian structure of such low Reynolds turbulence is likely to be very different from the prediction obtained in isotropic turbulence at high Reynolds numbers.

VII. CONCLUSIONS

In laboratory 2D turbulence, at modest Reynolds numbers (up to 200), fluid particles form coherent bundles which determine the statistics of the pair separation. This local anisotropy dominates both the pair separation and the exit time statistics bringing important deviations from statistical properties predicted in isotropic turbulence. We have recently shown that these bundles influence strongly turbulent mixing,[54] the transport of inertial particles,[55] or can even be utilized to design turbulence driven rotors[22] and self-propelled objects.[56]

ACKNOWLEDGMENTS

This work was supported by the Australian Research Council's Discovery Projects funding scheme (Nos. DP150103468 and DP160100863). H.X. acknowledges support from the Australian Research Council's Future Fellowship (No. FT140100067). N.F. acknowledges support by the Australian Research Council's DECRA Award (No. DE160100742). B.F. acknowledges support from the National Science Foundation under NSF Grant No. 1515202. The authors thank G. Falkovich and K. Szewc for useful discussions.

REFERENCES

[1] R. Kraichnan, "Inertial ranges in two-dimensional turbulence," Phys. Fluids **10**, 1417 (1967).

[2] D. K. Lilly, "Two-dimensional turbulence generated by energy sources at two scales," J. Atmos. Sci. **46**, 2026 (1989).

[3] L. Smith and V. Yakhot, "Finite-size effects in forced two-dimensional turbulence," J. Fluid Mech. **274**, 115 (1994).

[4] D. Byrne, H. Xia, and M. Shats, "Robust inverse energy cascade and turbulence structure in three-dimensional layers of fluid," Phys. Fluids **23**, 095109 (2011).

[5] H. Xia and N. Francois, "Two-dimensional turbulence in three-dimensional flows," Phys. Fluids **29**, 111107 (2017).

[6] J. Sommeria, "Experimental study of the two-dimensional inverse energy cascade in a square box," J. Fluid Mech. **170**, 139 (1986).

[7] J. Paret and P. Tabeling, "Experimental observation of the twodimensional inverse energy cascade," Phys. Rev. Lett. **79**, 4162 (1997).

[8] M. C. Jullien, J. Paret, and P. Tabeling, "Richardson pair dispersion in two-dimensional turbulence," Phys. Rev. Lett. **82**, 2872 (1999).

[9] H. Xia, H. Punzmann, G. Falkovich, and M. Shats, "Turbulence-condensate interaction in two dimensions," Phys. Rev. Lett. **101**, 194504 (2008).

[10] H. Xia, M. Shats, and G. Falkovich, "Spectrally condensed turbulence in thin layers," Phys. Fluids **21**, 125101 (2009).

[11] G. Boffetta, A. Celani, and M. Vergassola, "Inverse energy cascade in two-dimensional turbulence: Deviations from Gaussian behavior," Phys. Rev. E **61**, R29 (2000).

[12] G. Boffetta, "Energy and enstrophy fluxes in the double cascade of two-dimensional turbulence," J. Fluid Mech. **589**, 253 (2007).

[13] G. Boffetta and R. E. Ecke, "Two-dimensional turbulence," Annu. Rev. Fluid Mech. **44**, 427 (2012).

[14] G. Falkovich, G. Boffetta, M. Shats, and A. S. Lanotte, "Introduction to focus Issue: Two-Dimensional turbulence," Phys. Fluids **29**, 110901 (2017).

[15] L. F. Richardson, "Atmospheric diffusion shown on a distance-neighbour graph," Proc. R. Soc. A **110**, 709–737 (1926).
[16] A. Obukhov, "Spectral energy distribution in a turbulent flow," Izv. Akad., Nauk SSSR, Ser. Geogr. Geofiz. **5**, 453–466 (1941).
[17] Y. Couder, J. M. Chomaz, and M. Rabaud, "On the hydrodynamics of soap films," Physica D **37**, 384 (1989).
[18] H. Kellay, X.-I. Wu, and W. I. Goldburg, "Experiments with turbulent soap films," Phys. Rev. Lett. **74**, 3975 (1995).
[19] H. Kellay, T. Tran, W. I. Goldburg, N. Goldenfeld, G. Goia, and P. Chakraborty, "Testing a missing spectral link in turbulence," Phys. Rev. Lett. **109**, 254502 (2012).
[20] A. von Kameke, F. Huhn, G. Fernandez-Garcia, A. P. Munuzuri, and V. Perez-Munuzuri, "Double cascade turbulence and Richardson dispersion in a horizontal fluid flow induced by Faraday waves," Phys. Rev. Lett. **107**, 074502 (2011).
[21] N. Francois, H. Xia, H. Punzmann, and M. Shats, "Inverse energy cascade and emergence of large coherent vortices in turbulence driven by Faraday waves," Phys. Rev. Lett. **110**, 194501 (2013).
[22] N. Francois, H. Xia, H. Punzmann, and M. Shats, "Rectification of chaotic fluid motion in two-dimensional turbulence," Phys. Rev. Fluids **3**, 124602 (2018).
[23] H. Xia, N. Francois, H. Punzmann, and M. Shats, "Taylor particle dispersion during transition to fully developed two-dimensional turbulence," Phys. Rev. Lett. **112**, 104501 (2014).
[24] H. Xia, N. Francois, H. Punzmann, and M. Shats, "Lagrangian scale of particle dispersion in turbulence," Nat. Commun. **4**, 3013 (2013).
[25] N. Francois, H. Xia, H. Punzmann, S. Ramsden, and M. Shats, "Three-dimensional fluid motion in Faraday waves: Creation of vorticity and generation of two-dimensional turbulence," Phys. Rev. X **4**, 021021 (2014).
[26] H. Xia, D. Byrne, G. Falkovich, and M. Shats, "Upscale energy transfer in thick turbulent fluid layers," Nat. Phys. **7**, 321–324 (2011).
[27] M. Shats, D. Byrne, and H. Xia, "Turbulence decay rate as a measure of flow dimensionality," Phys. Rev. Lett. **105**, 264501 (2010).
[28] H. Punzmann, N. Francois, H. Xia, G. Falkovich, and M. Shats, "Generation and reversal of surface flows by propagating waves," Nat. Phys. **10**, 658 (2014).
[29] N. Francois, H. Xia, H. Punzmann, P. W. Fontana, and M. Shats, "Wave-based liquid-interface metamaterials," Nat. Commun. **8**, 14325 (2017).
[30] M. Shats, H. Xia, H. Punzmann, and G. Falkovich, "Suppression of turbulence by self-generated and imposed mean flows," Phys. Rev. Lett. **99**, 164502 (2007).
[31] H. Xia, T. Maimbourg, H. Punzmann, and M. Shats, "Oscillon dynamics and rogue wave generation in Faraday surface ripples," Phys. Rev. Lett. **109**, 114502 (2012).
[32] M. Shats, H. Xia, and H. Punzmann, "Parametrically excited water surface ripples as ensembles of oscillon," Phys. Rev. Lett. **108**, 034502 (2012).
[33] N. Francois, H. Xia, H. Punzmann, and M. Shats, "Wave-particle interaction in the Faraday waves," Eur. Phys. J. E **38**, 106 (2015).
[34] A. Celani, S. Musacchio, and D. Vincenzi, "Turbulence in more than two and less than three dimensions," Phys. Rev. Lett. **104**, 184506 (2010).
[35] J. R. Cressman, J. Davoudi, W. I. Goldburg, and J. Schumacher, "Eulerian and Lagrangian studies in surface flow turbulence," New J. Phys. **6**, 53 (2004).
[36] G. Boffetta and A. Celani, "Pair dispersion in turbulence," Physica A **280**, 1–9 (2000).
[37] G. Boffetta and I. M. Sokolov, "Statistics of two-particle dispersion in two-dimensional turbulence," Phys. Fluids **14**, 3224–3232 (2002).
[38] M. K. Rivera and R. E. Ecke, "Lagrangian dynamics in two-dimensional turbulence," Phys. Rev. Lett. **95**, 194503 (2005).
[39] T. Vicsek and A. Zafeiris, "Collective motion," Phys. Rep. **517**, 71 (2012).
[40] I. M. Sokolov and R. Reigada, "Dispersion of passive particles by a quasi-two-dimensional turbulent flow," Phys. Rev. E **59**, 5412 (1999).
[41] M. D. Finn and J. L. Thiffeault, "Topological optimisation of rod-stirring devices," SIAM Rev. **53**, 723 (2011).
[42] M. Allshouse and J. L. Thiffeault, "Detecting coherent structures using braids," Physica D **241**, 95–105 (2012).
[43] J. L. Thiffeault, "Braids of entangled particle trajectories," Chaos **20**, 017516 (2010).
[44] N. Francois, H. Xia, H. Punzmann, B. Faber, and M. Shats, "Braid entropy of two-dimensional turbulence," Sci. Rep. **5**, 18564 (2015).
[45] G. Falkovich, K. Gawedzki, and M. Vergassola, "Particles and fields in fluid turbulence," Rev. Mod. Phys. **73**, 913 (2001).
[46] H. Kellay and W. I. Goldburg, "Two-dimensional turbulence: A review of some recent experiments," Rep. Prog. Phys. **65**, 845 (2002).
[47] Z. Warhaft, "Passive scalars in turbulent flows," Annu. Rev. Fluid Mech. **32**, 203–224 (2000).
[48] J. P. L. C. Salazar and L. R. Collins, "Two-particle dispersion in isotropic turbulent flows," Annu. Rev. Fluid Mech. **41**, 405–432 (2009).
[49] M. Bourgoin, N. T. Ouellette, H. Xu, J. Berg, and E. Bodenschatz, "The role of pair dispersion in turbulent flow," Science **311**, 835 (2006).
[50] S. Goto and J. C. Vassilicos, "Particle pair diffusion and persistent streamline topology in two-dimensional turbulence," New J. Phys. **6**, 65 (2004).
[51] S. Thalabard, G. Krstulovic, and J. Bec, "Turbulent pair dispersion as a continuous-time random walk," J. Fluid Mech. **755**, R4-1 (2014).
[52] M. Bourgoin, "Turbulent pair dispersion as a ballistic cascade phenomenology," J. Fluid Mech. **772**, 678–704 (2015).
[53] G. Kokot, S. Das, R. G. Winkler, G. Gompper, I. S. Aranson, and A. Snezhko, "Active turbulence in a gas of self-assembled spinners," Proc. Natl. Acad. Sci. U. S. A. **114**, 12870–12875 (2017).
[54] H. Xia, N. Francois, H. Punzmann, K. Szewc, and M. Shats, "Extreme concentration fluctuations due to local reversibility of mixing in turbulent flows," Mod. Phys. Lett. B **32**, 1840028 (2018).
[55] H. Xia, N. Francois, H. Punzmann, and M. Shats, "Tunable diffusion in wave-driven two-dimensional turbulence," J. Fluid Mech. (in press).
[56] J. Yang, M. Davoodianidalik, H. Xia, H. Punzmann, M. Shats, and N. Francois, "Passive swimming in hydrodynamic turbulence at a fluid surface," Phys. Rev. Fluids (submitted).